Research Article

Fredselin R. S. Vithel, Ramadoss Manimekalai*, Sreekrishnan Rajammal Cynthia, Vediyappan Govindan, M. Ijaz Khan, Sherzod Abdullaev, Salman A. AlQahtani*, and Nouf F. AlQahtani*

Growth, characterization, and anti-bacterial activity of L-methionine supplemented with sulphamic acid single crystals

https://doi.org/10.1515/phys-2023-0175 received July 13, 2023; accepted December 20, 2023

Abstract: Sulphamic acid (SA) crystals supplemented with L-methionine (LM) were grown at moderate temperatures using a slow evaporation procedure. The powder XRD pattern showed that LM supplemented with SA (LMSA) crystals have an orthorhombic crystal structure. The FTIR studies confirmed the presence of various vibrational modes. Using a UV-Vis spectrometer, the transmittance of LMSA in the UV and visible range was observed, and the band gap of the LMSA was also calculated. The hardness value of LMSA was higher compared to that of pure SA. Photoluminescence emission studies of LMSA pointed out emissions at 491 and 542 nm, which were attributed to the transition from the 5D_4

state to 7F_6 and 7F_5 ground, respectively. LMSA crystals were effective in killing pathogenic bacteria, according to the studies on their anti-bacterial activity.

Keywords: powder XRD, FTIR studies, orthorhombic crystal structure, L-methionine, SA crystals

1 Introduction

The creation of passive and active photonic devices primarily makes use of non-linear optical materials [1]. Optics and electronics are two fields where the utilization of single crystals is evident [2]. Sulphamic acid (H2NSO3H, SA) is one of the most generally used inorganic compounds in industry [3]. It is now used in place of traditional Lewis and Bronsted acid catalysts. SA is a white-coloured, odourless, crystalline solid, and is non-corrosive, non-volatile, and non-hygroscopic. It is also a very effective green catalyst in organic synthesis [4] and a potent inorganic acid that assumes a zwitterionic form when combined with water. Because of these benefits, the British Analytical Methods Committee and IUPAC, as well as the Japanese Industrial Standard, suggested SA as a benchmark ingredient in titrimetric testing [5]. In multistage flash evaporation desalination plants, SA identifies good applications for heat exchangers, demisters, cleaning, cooling water systems, etc. [2]. The orthorhombic structure and zwitterionic form of sulphuric acid are present. Various reports have suggested the formation of SA in the shape of single crystals at moderate temperatures [6-10]. Numerous researchers have shown interest in SA crystals, and different combinations of these crystals have been synthesized, and their properties have been reported [11–28]. SA has been utilized in many applications, especially in polymerization, and utilized as a catalyst in many organic reactions. It is employed as a herbicide, cross-linking agent in polymer synthesis, a fire retardant or fireproofing agent, a fabric dyer, an air

e-mail: maniabi64@gmail.com

Fredselin R. S. Vithel: Department of Physics, A.V.V.M. Sripushpam College, Poondi, Thanjavur, Affiliated to Bharathidasan University, Tamil Nadu, India, e-mail: fredselin@yahoo.com

Sreekrishnan Rajammal Cynthia: Department of Physics, Alagappa Chettiar Government College of Engineering and Technology, Karaikudi, Tamil Nadu, India, e-mail: srcynthiasam@gmail.com

Vediyappan Govindan: Department of Mathematics, Hindustan Institute of Technology and Science (Deemed to be University), Padur, Kelambakkam, 603103, India

M. Ijaz Khan: Department of Mechanics and Engineering Science, Peking University, Beijing, 100871, China, e-mail: 2106391391@pku.edu.cn Sherzod Abdullaev: Faculty of Chemical Engineering, New Uzbekistan University, Tashkent, Uzbekistan; Engineering School, Central Asian University, Tashkent, Uzbekistan, e-mail: sherzodbek.abdullaev.1001@gmail.com

^{*} Corresponding author: Ramadoss Manimekalai, Department of Physics, A.V.V.M. Sripushpam College, Poondi, Thanjavur, Affiliated to Bharathidasan University, Tamil Nadu, India,

^{*} Corresponding author: Salman A. AlQahtani, Computer Engineering Department, College of Computer and Information Sciences, King Saud University, Riyadh, Saudi Arabia, e-mail: salmanq@ksu.edu.sa

^{*} Corresponding author: Nouf F. AlQahtani, Islamic Studies Department, College of Education, King Saud University, Riyadh, Saudi Arabia, e-mail: noufff@ksu.edu.sa

2 — Fredselin R. S. Vithel *et al.* DE GRUYTER

cleaner, a pulp bleaching agent, a scale remover and metal cleaner, a pigment printer, and to make less toxic cigarettes [29]. L-Methionine (LM) is an α -amino acid that possesses a protonated amino group (NH₃), S-methyl thioether side chain, and deprotonated carboxylic acid group (COO). As a precursor, LM takes part in the biosynthesis of proteins. It is categorized as an aliphatic and non-polar amino acid. The primary characteristic of LM and some of its metal compounds is their catalytic activity, which confers precise antiviral effects. This amino acid is converted into creatine monohydrate, which is a material required for the production of energy and muscle growth [30]. Here, we report the growth of LM supplemented with SA (LMSA) (single crystals), its structural and optical properties, and its anti-bacterial activity.

2 Experimental methods

SA crystals containing LM were produced utilizing the slow evaporation method. LM powder and high-purity SA were employed as the initial components. Both LM and SAs were purchased from Sigma-Aldrich (reagent grade \geq 98%). The saturated aqueous solution of 1,000 ml was prepared using recrystallization SA (NH₂SO₃H) and LM SA (C₅H₁₁NO₂S) in a ratio of 3:1 with distilled water at 35°C. At room temperature, the dissolved solution was agitated with a magnetic stirrer for 2–3 h, and a clear solution was obtained. The prepared translucent and saturated solution was then filtered *via* filter paper. Then, the resultant solution was closed using a perforated polythene sheet to crystallize at moderate temperatures with a decontaminate surrounding. Good, colourless, and transparent crystals were obtained after 20 days and were used for characterization.

The stoichiometric equations for the formation of LMSA are as follows:

$$H_3NSO_3 + H_2O \rightarrow (NH_4)HSO_4,$$

 $(NH_4)HSO_4 + C_5H_{11}NO_2S \rightarrow C_5H_{14}N_2O_6S_2.$

Figure 1 depicts an image of the grown LMSA crystal. The anti-bacterial effect of LMSA crystals was determined with Gram-positive and Gram-negative bacteria using the disk diffusion Kirby–Bauer method. This test was conducted with a Mueller–Hinton agar medium. During this study, the antimicrobial-impregnated discs were positioned on the surface and incubated for 24 h at 35°C. Following incubation, a zone of inhibition corresponding to the degree of antimicrobial activity on the bacteria was observed on the plates. Any zone of inhibition that is observed suggests a level of susceptibility to the antibiotic; the bigger the zone, the

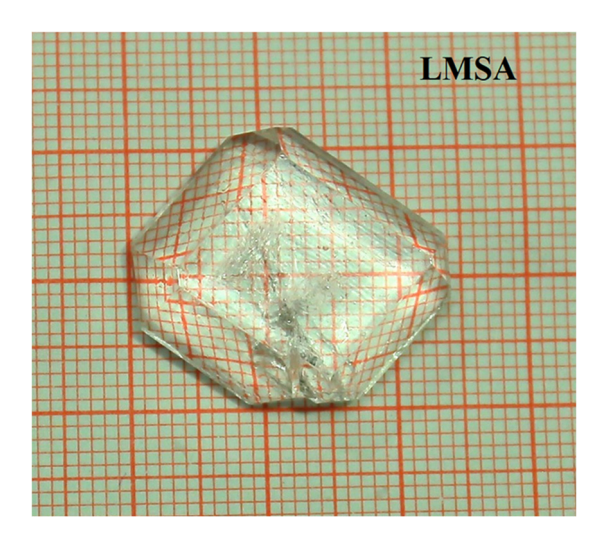


Figure 1: Image of LMSA crystal.

stronger the antibiotic. Conversely, the absence of any zone signifies complete resistance to germs. Afterwards, the diameter of the inhibition zone from the disc centre was measured, and the result was compared with the standard set of values to find the susceptibility of the bacteria in LMSA.

3 Results and discussion

3.1 X-ray diffraction

The XRD patterns of the SA crystal and SALM are shown in Figure 2. The XRD profile's diffraction peaks are compared with the accepted JCPDS data (JCPDS Card No.: 70-0060) of the pure SA crystal. For the pure SA crystal, a high-intensity peak was observed along the (2 2 1) direction. The XRD pattern of LMSA samples shows a high-intensity peak along the (102) direction. In addition, the strength of the strongest peak (211) and other peaks also reduced. The variation in the relative intensities of the different peaks was also discovered, which indicated that LM had been added to the pure SA. The single XRD and powder XRD patterns reveal that the synthesized LMSA possess orthorhombic crystal structures with reduced cell volume (Table 1).

3.2 FT-IR analysis

Figure 3 displays the FT-IR spectrum of the grown crystals (LMSA). The spectrum reveals the NH_3^+ mode of bonding existing at frequencies 3,153 and 2,872 cm $^{-1}$. Triband overtones and a combination of hydrogen-bonded OH bending modes were responsible for the bands observed at 2,449 and 2,026 cm $^{-1}$. The bands observed at 1,807 and 1,451 cm $^{-1}$ were

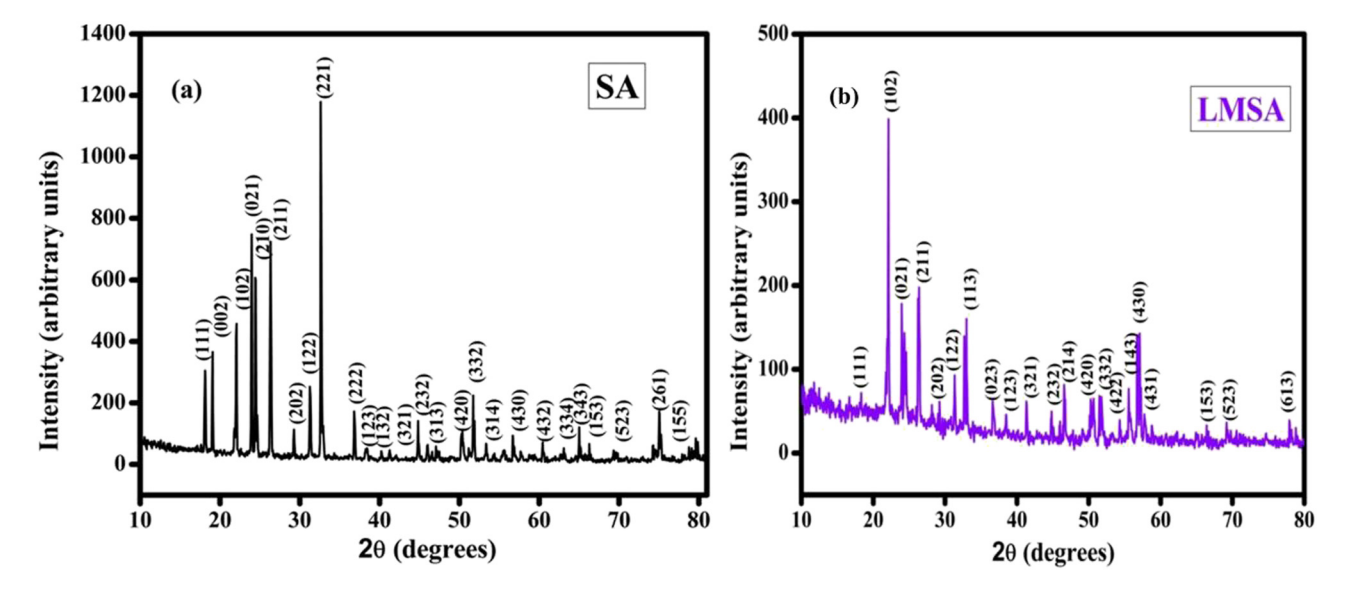


Figure 2: X-ray diffraction of SA and LMSA crystal.

attributed to the NH₃⁺ mode of vibration deforming, while the mode at 1,066 cm⁻¹ was attributed to symmetric SO₃ stretching, and the vibration bands found at 1,285 cm⁻¹ were due to degenerated SO₃ stretching. The generation of zwitterions in SA and LMSA crystals was verified by the presence of the rocking mode vibration of NH₃⁺ at 1,002 cm⁻¹ [26].

The N-S stretching vibration at 695 cm⁻¹ was observed, while the band at 536 cm⁻¹ was due to the degraded SO₃⁻ deformation [6]. All of the IR bands that appeared in the grown crystals were analogues of bands that had been theoretically computed and were in excellent accordance with previous studies [26,31]. The observed wave numbers and the corresponding assignments of SA and LMSA are listed in Table 2. However, nearly all of the modes were apparent in LM-supplemented crystals. However, there was a small variation in the intensities, indicating that the sublattice geometry may have slightly changed.

3.3 UV-Vis studies

Considering that the formed crystals are used in a variety of optoelectronic device applications, it is crucial to understand

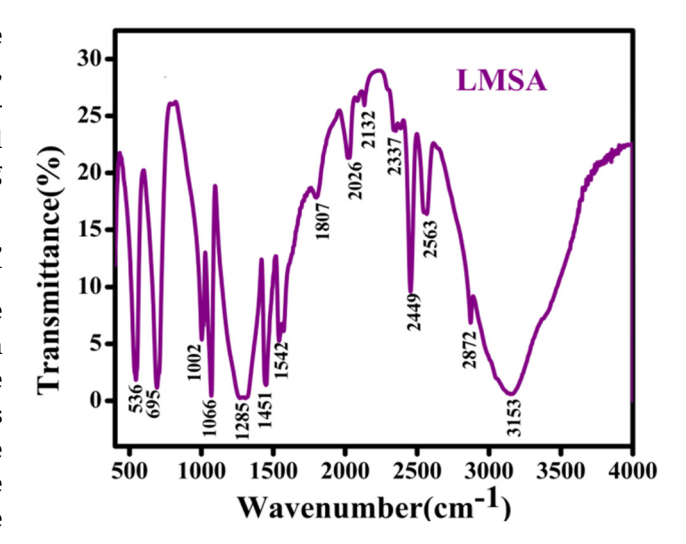


Figure 3: FTIR spectrum of LMSA.

the optical transparency of these materials. Figure 4 shows the transmittance spectrum of LMSA and indicates that the prepared crystals are 98% transparent. Because of their increased crystalline nature, LMSA crystals are more transparent. According to Senthil Pandian et al. [32], the scattering from point and line defects is likely the cause of the decrease

Table 1: Lattice parameters and structures of SA and LMSA

| Sample | a (A°) | b (A°) | c (A°) | $\alpha = \beta = y$ | Volume (A ³) | Structure |
|--------|--------|--------|--------|----------------------|--------------------------|--------------|
| SA | 8.1266 | 8.0928 | 9.2298 | 90° | 607.0166 | Orthorhombic |
| LMSA | 8.1311 | 8.0695 | 9.2362 | 90° | 606.0270 | Orthorhombic |

Table 2: Vibrational assignment of LMSA

| Wave number (cm ⁻¹) | Assignment | | |
|---------------------------------|---|--|--|
| LMSA | | | |
| 3,153 | Degenerated NH ₃ stretching | | |
| 2,872 | Symmetric NH ₃ stretching | | |
| 2,449 | S–H stretching | | |
| 2,026 | N–H stretching | | |
| 1,807 | Symmetric NH ₃ +deformation | | |
| 1,542 | Degenerated NH ₃ deformation | | |
| 1,451 | Symmetric NH ₃ deformation | | |
| 1,285 | Degenerated SO ₃ stretching | | |
| 1,066 | Symmetric SO ₃ stretching | | |
| 1,002 | Rocking mode NH ₃ ⁺ | | |
| 695 | N-S stretching | | |
| 536 | Degenerated SO ₃ deformation | | |
| | | | |

in transmittance in SA crystals. As shown in Figure 5, LMSA shows a lower UV cutoff wavelength of 263 nm, which indicates that LMSA has a higher percentage of absorption than that of pure SA [33]. To determine the band gap energy value, a Tauc plot analysis was conducted, as shown in Figure 6, and the optical energy band gap of LMSA was calculated to be 3.5 eV.

3.4 Vickers hardness test

The effectiveness of crystals depends mostly on their optical properties and sound mechanical behaviour [25,26]. At room temperature, the Vickers microhardness measurements were conducted on LMSA crystals with loads ranging

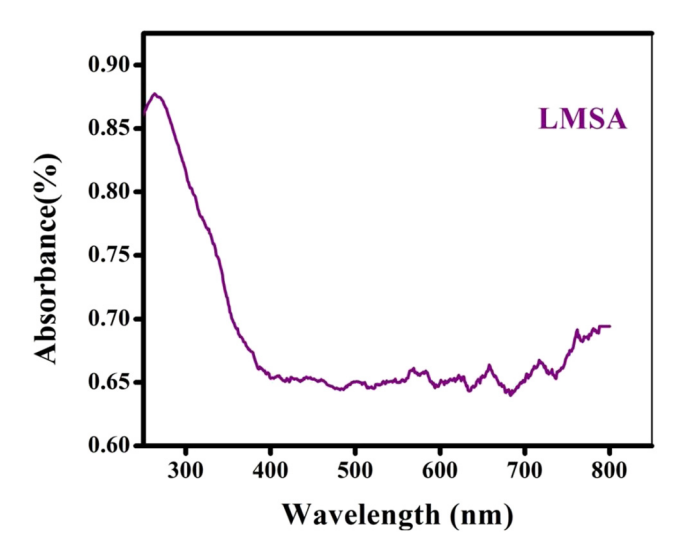


Figure 5: UV absorption of LMSA crystal.

from 25 to 100 g. For different utilized loads p (in g), the indentation diagonal lengths d (in m) were measured. The Vickers hardness number was derived by the following relationship:

$$Hv = 1.8544P/d^2 \text{ kg mm}^{-2}$$
.

The curve between the load and hardness number is shown in Figure 7. Up to 100 g, with an increase in the load, the hardness value increased; however, no break was spotted in the plot. The LMSA crystals showed an enhanced hardness in the presence of LM. Arumugam *et al.* [33] and Ramesh Babu *et al.* [12] also noted the same behaviour. Figure 8 depicts the outcomes of measuring the work hardening coefficient from the plot of log *p vs* log *d.* The straight

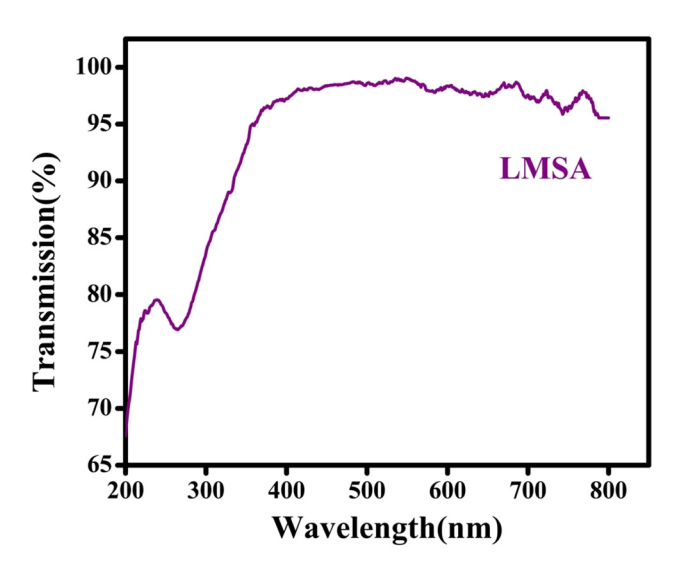


Figure 4: UV transmission spectrum of LMSA crystal.

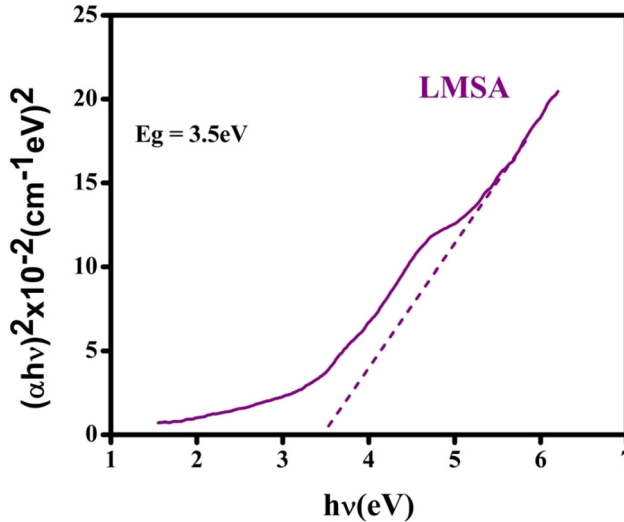


Figure 6: Tauc's plot of LMSA.

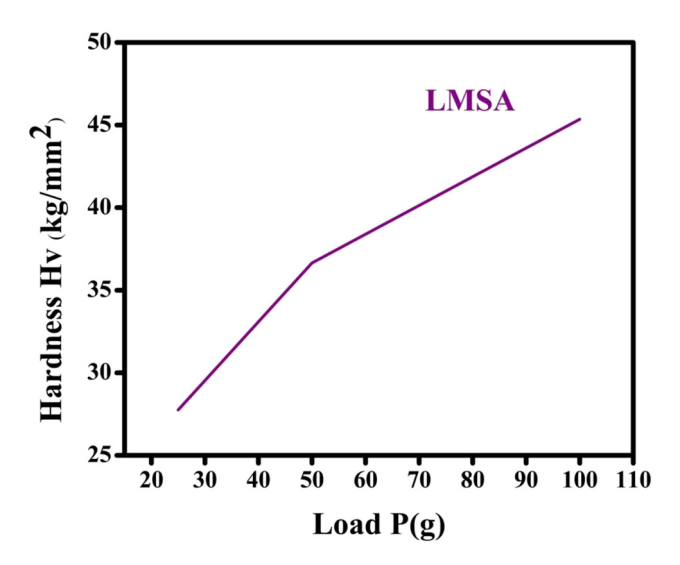


Figure 7: Load P and hardness number of LMSA.

line produced by the least-squares fitting was in fine agreement with Meyer's law. The value of n was obtained from the slope. In line with Senthilkumar *et al.* [33], *n* needs to be above 1.6 for soft materials and between 1 and 1.6 for hard materials. Since n is above 1.6 for the LMSA crystal, it is considered a soft material.

3.5 Photoluminescence studies

Figure 9 displays the LMSA crystal's emission spectrum, which revealed emissions in the visible and ultraviolet zones. In the visible area, emissions of green, blue, and violet are observed. A strong blue emission, observed at 491 nm, is the strongest among all the detected emissions.

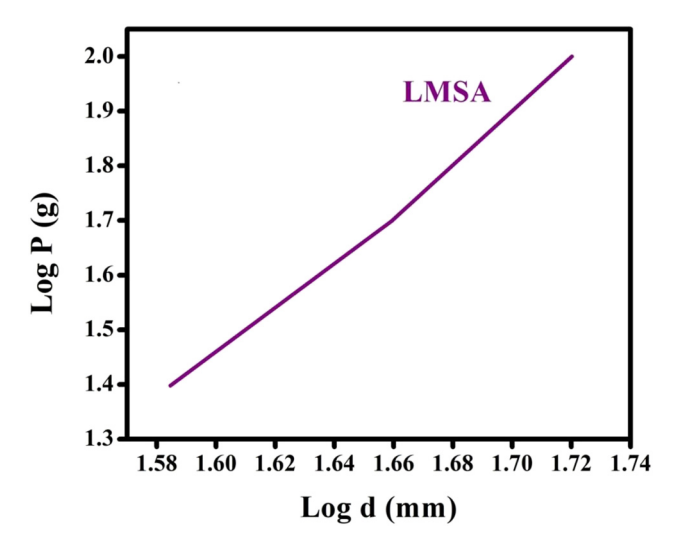


Figure 8: Log P and Log D of LMSA.

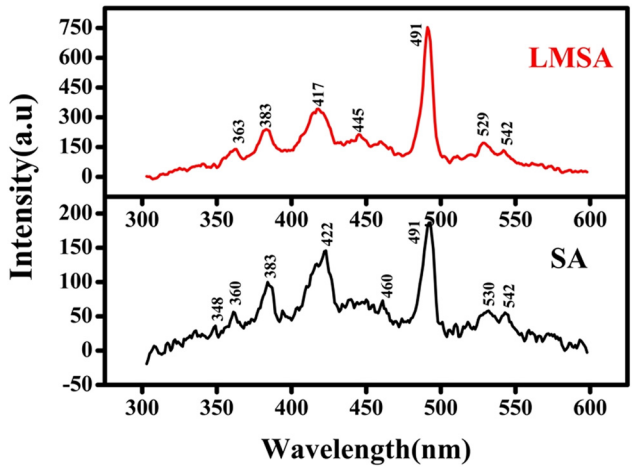


Figure 9: Photo luminescence spectrum of SA and LMSA.

According to Arumugam et al. [34], the peaks in the ultraviolet area that are noticed below 400 nm were caused by the electronic transition $\pi^-\pi^+$. The peaks observed at wavelengths below 500 nm resembled blue emission [35]. These emissions were caused by the transition between the energy levels 5D_4 to 7F_6 . The transition from 5D_4 to 7F_5 energy levels caused the peak at 529 nm to be associated with green emission [24]. A close inspection reveals an improvement in the blue emission intensity. This crystal can be used in blue-emission optoelectronic devices in the future due to its strong blue-emission properties [36]. Sun et al. [41], Wang et al. [42], and Zhang et al. [43] highlight the physical importance of low molecular weight polysaccharides from Dendrobium officinale, the surface-functionalized design of blood-contacting biomaterials, and the behaviour of environmental pH on the interaction characteristics of WP-EGCG non-covalent nano-complexes. Cui et al. [44], Zhao et al. [45], and Xu et al. [46] scrutinized the characterization and synthesis of Eu (III) complexes of modified cellulose and found an efficient reduction of betalactoglobulin allergenicity and that royal jelly acid suppresses hepatocellular carcinoma tumourigenicity, respectively. Selective enrichment of partial denitrifying bacteria, partial

Table 3: Anti-bacterial effect of LMSA crystals

| Name of bacteria | Inhibition zone of LMSA (mm) | Inhibition zone of the standard antibiotic Amikacin (mm) |
|---------------------|---------------------------------|--|
| S. aureus | 35 | 22 |
| B. klebsiella | 32 | 20 |
| E. coli | 35 | 22 |
| Serattia | 32 | 19 |

6 — Fredselin R. S. Vithel *et al.* DE GRUYTER

Table 4: Inhibition zone of LMSA compared with other reported materials

| Materials | Bacteria name | Zone of inhibition (mm) | Ref. |
|---|---------------|-------------------------|--------------|
| MSA | E. coli | 35 | Present work |
| | S. aureus | 35 | |
| Piper betle | E. coli | 22.5 | [37] |
| | S. aureus | 15.3 | |
| LTSB (L-threoninum sodium bromide) | E. coli | 15 | [38] |
| | S. aureus | 12 | |
| f6-(1,3-Benzodioxol-5-ylmethyl)-5-ethyl-2-{[2-(morpholin-4-yl)ethyl]sulfanyl} pyrimidin-4(3H)-one | S. aureus | 20 | [39] |
| Ferulic acid crystals | E. coli | 20 | [40] |

nitrification-anammox, and sulphur autotrophic denitrification in one reactor and cinnamic hydroxamic acid collector, as well as the examination of flotation attributes and the appliance of scheelite, has been recently discussed by Ahmad *et al.* [47], Zhao *et al.* [48], and Yao *et al.* [49], respectively.

3.6 Anti-bacterial activity

Using the disk diffusion Kirby–Bauer method, the anti-bacterial effect of LMSA was investigated against *Staphylococcus aureus* and *Bacillus*, which were Gram-positive, and *Klebsiella*, *Escherichia coli*, and *Serattia*, which were Gram-negative. The Mueller–Hinton agar medium was used in the disk diffusion test.

The recognized normal antibiotic half-life of *E. coli* is 22 mm; however, in LMSA, it was lengthened. The other bacteria, such as *S. aureus*, *Bacillus*, *Klebsiella*, and *Serattia*, also showed a lengthened inhibition zone compared to the inhibition zone of the standard antibiotic. Table 3 shows the antibacterial effect of the LMSA crystal. The anti-bacterial effect of LMSA is compared with other reported materials and is given in Table 4. From this, we deduced that the produced crystals were more potent than conventional and recently developed antibiotic materials.

4 Conclusion

At room temperature, slow evaporation was used to grow SA crystals and crystals containing LM. The structure of the grown crystals and lattice constants were validated by powder XRD. When LM was added to SA, a modest change in the crystal's lattice properties and volume was observed. When LM was added to SA, there was no discernible phase shift. The vibrational modes of the LMSA crystals were analysed using FTIR. The infrared bands observed in the

grown crystals were all theoretically computed bands that matched well with those in previous research. The optical studies verified that LMSA crystals become more transparent due to their increasing crystalline nature. The band gap value of the LMSA crystal was calculated to be 3.5 eV. The addition of LM enhanced the mechanical strength of the crystal. The greatest peak in the photoluminescence experiments that resulted from the 5D_4 to 7F_6 transition reveals blue emission. Thus, the grown crystals open the door to future use of these crystals in blue emission optoelectrical systems. The enriched anti-bacterial effect of the LMSA confirms that this crystal will be a promising material for eliminating harmful microorganisms.

Acknowledgments: The authors acknowledge the support by Research Supporting Project Number (RSPD2024R585), King Saud University, Riyadh, Saudi Arabia.

Funding information: This work was supported by Research Supporting Project Number (RSPD2024R585), King Saud University, Riyadh, Saudi Arabia.

Author contributions: All authors have accepted responsibility for the entire content of this manuscript and approved its submission.

Conflict of interest: The authors state no conflict of interest.

Data availability statement: Data sharing is not applicable to this article as no datasets were generated or analysed during the current study.

References

[1] Ramesh Babu R, Sethuraman K, Vijayan N, Gopalakrishnan R, Ramasamy P. Dielectric and structural studies on sulphamic acid (SA) single crystal. Mater Lett. 2007;61:3480-5.

- [2] Shakir M, Riscob B, Ganesh V, Vijayan N, Gupta R, Plaza J, et al. Crystal growth, structural, crystalline, perfection, optical and mechanical properties of Nd3 + doped sulfamic acid(SA) single crystals. J Cryst Growth. 2013;380:228-35.
- [3] Wong MW, Kenneth B, Michael JF. Solvent effects. 2. Medium effect on the structure energy charge density, and vibrational frequencies of sulphamic acid. J Am Chem Soc. 1992;114:523-9.
- Marcelo G. Montes D. Soares RM. Moura RR. Granião VF. Sulfamic acid: An efficient acid catalyst for esterification of FFA. Fuel. 2012;97:884-6.
- Jaishree D, Kanchana G, Kesavasamy R. Synthesis growth and characterization of magnesium sulphamate - A promising nonlinear optical crystal. Indian J Pure Appl Phys. 2015;53:404-8.
- Valluvan R. Selvaraiu K. Kumararaman S. Growth and characterization of sulphamic acid single crystals: A non-linear optical material. Mater Chem Phys. 2006;97:81-4.
- Yohimori T, Tanaka T. Preparation of sulphamic acid single crystals and their assay by precise coulometric titration. Anal Chem Acta.
- Anupriya KG, Hemalatha P. Effect of Znso4 and M nso4 on the growth of sulphamic acid single crystals. Mat Sci Res India. 2018;15:151-8.
- Kanda FA, King AJ. The crystal structure of sulfamic acid. J Am Chem Soc. 1951;73(5):2315-9.
- [10] Cheng LK, Bosenberg WR, Tang CL. Growth and characterization of nonlinear optical crystals suitable for frequency conversion. Prog Cryst Growth Charact Mater. 1990;20:9-57.
- [11] Shakir M, Riscob B, Ganesh V, Vijayan N, Gupta R, Plaza J, et al. Crystal growth, structural, crystalline, perfection, optical and mechanical properties of Nd3 + doped sulfamic acid(SA) single crystals. J Cryst Growth. 2013;380:228-35.
- Ramesh Babu R, Ramesh R, Gopalkrishnan R, Ramamurthi K, Bhagavanarayana G. Growth, structural, spectral, mechanical and optical properties of pure and metal ions doped sulphamic acid single crystals. Spectrochim Acta Part A Mol Biomol Spectrosc. 2010:76:470-5.
- [13] Thaila T, Kumararaman S. Effect of Nacl and Kcl doping on the growth of sulphamic acid crystals. Spectrochim Acta Part A Mol Biomol Spectrosc. 2011;82:20-4.
- [14] Sass RL. A neutron diffraction study on the crystal structure of sulfamic acid. Acta Crystallogr. 1960;13:320-4.
- [15] Kannan BR, Seshadri P, Murugakoothan P, Illangovan K. Growth and characterisation of lanthanum doped sulphamic acid single crystal. Indian J Sci Technol. 2013;6:4357-61.
- [16] Kannan BR, Seshadri P, Illangovan K, Murugakoothan P. Growth and characterisation of thiourea doped sulphamic acid single crystals. Indian J Sci Technol. 2013;6:4908-11.
- [17] Kannan B, Seshadri PR, Illangovan K, Murugakoothan P, Illangovan K. Effect of neodymium on the growth of sulphamic acid single crystal. Indian J Sci Technol. 2014;7:221.
- [18] Anupriya K, Hemalatha P, Arunadevi N. Growth and characterization of aluminium nitrate doped sulphamic acid single crystal. Int Innov Res Sci Eng Technol. 2017;6:8254.
- [19] Brahmaji B, Rajyalakshmi S, Kamal CS, Atla V, Veeraiah V, Rao KV, et al. Optical emissions of Ce³⁺ doped Sulphamic acid single crystals by low temperature unidirectional growth technique. Opt Mat. 2017;64:100-5.
- [20] Kannan BR, Seshadri P, Murugakoothan P, Illangovan K. Growth and characterisation of gudolinium doped sulphamic acid single crystal. Int J Chem Tech Res. 2014;6:1168-73.

- [21] Kannan BR, Seshadri P, Murugakoothan P, Illangovan K. Growth and characterization of yttrium doped sulphamic acid single crystal. Arch Phys Res. 2014;5:79-83.
- [22] Anupriya KG, Hemalatha P. Material science research india sulphamic acid single materials. 2018;15:151-8.
- Yesuvadian S, Selvaraj A, Methodius MM, Godavarti B, Narayanasamy V, Devarajan PA. Synthesis, growth and characterization of nitramino sulphonic acid (NASA) NLO single crystals. Optik. 2015;126:95-100.
- [24] Brahmaji B, Rajyalakshmi S, Visweswara Rao TK, Valluru SR, Esub Basha SK, Satyakamal Ch, et al. Tb³⁺ added sulfamic acid single crystals with optimal photoluminescence properties for opto-electric devices. J Sci: Adv Mater Dev. 2018;3:68-76.
- [25] Indumathi N, Chinnasamy E, Arulmani S, Venkatesan A, Saravanan M, Deepa K, et al. Third order nonlinear optical and electrical properties of new sulphamic acid lithium chloride single crystal. Mater Today: Proc. 2020;21:24-9.
- [26] Sing B, Shkir Mohd, Alfaiyb S, Kaushal A, Nasani N, Bdikin I, et al. Structural, optical, thermal, mechanical and dielectric studies of Sulfamic acid single crystals: An influence of dysprosium (Dy³⁺) doping. | Mol Struct. 2016;1119:365-72.
- Brahmaji B, Rajyalakshmi S, Satyakamal Ch, Veeraiah V, Ramachandra [27] Rao K, Atla V, et al. Optical emissions of Ce³⁺ doped Sulphamic acid single crystals by low temperature unidirectional growth technique. Opt Mater. 2017;64:100-5.
- Rafi Ahamed S, Srinivasan P. Synthesis, growth and characteriza-[28] tions of cesium sulfamate single crystal by solution growth technique. Elixir Cryst Growth. 2012;50:10628-31.
- Anthony Benson G, Spillane WJ. Sulfamic acid and its N-substituted [29] derivatives. Chem Rev. 1980;80:151-86.
- Shalini M, Sundararajan RS, Manikandan E, Meena M, Ebinezer MS, Sabari Girisun TC, et al. Growth and characterization of L-Methionine Barium Bromide (LMBB) semi-organic crystal for optical limiting applications. Optik. 2023;278:170705.
- [31] Haupa K, Bil A, Mielke Z. Donar-acceptor complexes between ammonia and sulfur trioxide: An FTIR and computational study. J Phys Chem A. 2015;119:10724-34.
- [32] Senthil Pandian M, Charoen In U, Ramasamy P, Manyum P, Lenin M, Balamurugan N. Unidirectional growth of sulphamic acid single crystal and its quality analysis using etching, microhardness, HRXRD, UV-visible and thermogravimetric-differential thermal characterizations. J Cryst Growth. 2010;312:397-401.
- [33] Senthilkumar K, Moorthy Babu S, Kumar B. Influence of dopants on Vickers microhardness of ferroelectric glycine phosphate single crystals. Proc Indian Natl Sci Acad. 2013;79:423-6.
- [34] Arumugam J, Suresh N, Selvapandiyan M, Sudhakar S, Prasath M. Effect of Nacl on the properties of sulphamic acid single crystals. Heliyon. 2019;5:e01988.
- [35] Sonia J, Vijayan N, Bhushan N, Thukral K, Raj K, Maurya KK, et al. Growth of a bulk-size single crystal of sulphamic acid by an inhouse developed seed rotation solution growth technique and its characterization. J Appl Cryst. 2017;50:763-8.
- Mansour N, Momeni A, Karimzadeh R, Amini M. Blue-green lumi-[36] nescent silicon nanocrystals fabricated by nanosecond pulsed laser ablation in dimethyl sulfoxide. Opt Mater Express. 2012;2:740-8.
- Ngamsurach P, Praipipat P. Anti-bacterial activities against Staphylococcus aureus and Escherichia coli of extracted Piper betle leaf materials by disc diffusion assay and batch experiments. RSC Adv. 2022;12:26435-54.

- [38] Ashvin Santhia SV, Aneeba B, Vinu S, Sheela Christy R, Al-Mohaimeed AM, Al Farraj DA. Studies on physicochemical and antibacterial deeds of amino acid based L-Threoninum sodium bromide. Saudi J Biol Sci. 2020;27:2987–92.
- [39] Attia MI, El-Brollosy NR, Kansoh Hazem AL, Ghabbour A, Al-Wabli RI, Fun H-K. Synthesis, single crystal X-ray structure, and antimicrobial activity of 6-(1, 3-benzodioxol-5-ylmethyl)-5-ethyl-2-{[2-(morpholin-4-yl)ethyl]sulfanyl}pyrimidin-4(3H)-one. J Chem. 2014:2014:1–8.
- [40] Sangeetha M, Mathammal R. Studies on the growth, characterization, physicochemical properties and anti-bacterial activity of ferulic acid crystals. Int J Pharm Sci. 2015;8:121–6.
- [41] Sun SJ, Deng P, Peng CE, Ji HY, Mao LF, Peng LZ. Extraction, structure and immunoregulatory activity of low molecular weight polysaccharide from dendrobium officinale. Polymers. 2022;14:2899.
- [42] Wang Y, Zhai W, Cheng S. Surface-functionalized design of blood-contacting biomaterials for preventing coagulation and promoting hemostasis. Friction. 2023;11:1371–94.
- [43] Zhang S, Dongye Z, Wang L, Li Z, Kang M, Qian Y, et al. Influence of environmental pH on the interaction properties of WP-EGCG non-covalent nanocomplexes. J Sci Food Agric. 2022;103:5364–75.

- [44] Cui G, Li Y, Shi T, Gao Z, Qiu N, Satoh T, et al. Synthesis and characterization of Eu(III) complexes of modified cellulose and poly (N-isopropylacrylamide). Carbohydr Polym. 2023;94:77–81.
- [45] Zhao Q, Wang Y, Zhu Z, Zhao Q, Zhu L, Jiang L. Efficient reduction of β-lactoglobulin allergenicity in milk using Clostridium tyrobutyricum Z816. Food Sci Hum Wellness. 2023;12:809–16.
- [46] Xu H, Li L, Wang S, Wang Z, Qu L, Wang C, et al. Royal jelly acid suppresses hepatocellular carcinoma tumorigenicity by inhibiting H3 histone lactylation at H3K9la and H3K14la sites. Phytomedicine. 2023;118:154940.
- [47] Ahmad HA, Ahmad S, Gao L, Ismail S, Wang Z, El-Baz A, et al. Multiomics analysis revealed the selective enrichment of partial denitrifying bacteria for the stable coupling of partial-denitrification and anammox process under the influence of low strength magnetic field. Water Res. 2023;245:120619.
- [48] Zhao Y, Dong Y, Chen X, Wang Z, Cui Z, Ni Z. Using sulfide as nitrite oxidizing bacteria inhibitor for the successful coupling of partial nitrification-anammox and sulfur autotrophic denitrification in one reactor. Chem Eng J. 2023;475:146286.
- [49] Yao X, Yu X, Wang L, Zeng Y, Mao L, Liu S, et al. Preparation of cinnamic hydroxamic acid collector and study on flotation characteristics and mechanism of scheelite. Int J Min Sci Technol. 2023;33:773–81.